ELSEVIER

Catalysis Today 56 (2000) 315–324

CATALYSIS TODAY

www.elsevier.com/locate/cattod

# Measurements of surface exchange kinetics and chemical diffusion in dense oxygen selective membranes

Rune Bredesen [a,*], Frédéric Mertins [a], Truls Norby [b]

[a] *SINTEF Materials Technology, PO Box 124 Blindern, N-0314 Oslo, Norway*

[b] *Centre for Materials Science, University of Oslo, Gaustadalléen 21, N-0349 Oslo, Norway*

**Abstract**

The values of the chemical diffusion coefficient ($D$) and the surface exchange reaction rate constant ($k$) for the incorporation of oxygen in air, have been determined in $Sr_{4-x}La_xFe_{6-y}Ti_yO_{13+(x+y)/2}$ by transient thermogravimetric measurements at 700–1000°C. Only minor changes in the values of $D$ have been observed on doping $Sr_4Fe_6O_{13}$ with La and/or Ti. It is suggested that the concentration of interstitial oxygen ions is mainly determined by the inherent properties of the material, and that doping with 10% La and 6.7% Ti on the A- and B-sites do not give significant changes. An activation energy in the range 50–130 kJ mol$^{-1}$ was found for $D$. The values of $k$ were found to be nearly independent of the temperature. $k$ is approximately two orders of magnitude larger than $D$ suggesting that the surface kinetics is only rate limiting in the initial stage of the measurements. 

*Keywords:* Transient thermogravimetric measurements; Chemical diffusion coefficient; Surface exchange rate constant; Pure and La- and Ti-doped $Sr_4Fe_6O_{13}$

## 1. Introduction

Oxygen conducting membranes have been intensively studied during the last 10 years due to their use as electrolytes in solid oxide fuel cells (SOFCs). The main membrane materials developed for such applications are the fluorites Y-doped $ZrO_2$ and Gd-doped $CeO_2$. SOFCs are mainly used for electricity generation, but may also be used as oxygen pump for pure oxygen production. A drawback of the SOFC technology is the complex cell configuration comprising in addition to the electrolyte, anode and cathode electrodes, and interconnect materials. The problems of integration of these components at high temperature are the main reason for the lacking of an industrial breakthrough.

During the recent years mixed oxygen ion and electron conducting materials for use as dense oxygen selective membranes have received increasing interest in academia and industry. Due to the simultaneous transport of oxygen ions and electrons in these materials there is no need for an external electronic circuit, i.e., the electrodes can be avoided, and the membrane configuration consists only of the oxide wall. The difference between a fuel cell configuration containing an oxygen ion electrolyte and a mixed conducting membrane configuration is illustrated in Fig. 1.

The simplicity of the mixed conducting membrane configuration makes this type of membrane much more attractive for pure oxygen production than the electrolyte type based on the SOFC concept. Furthermore, during the last 4 years high oxygen flux and

* Corresponding author. Fax: +47-2206-7350.
*E-mail address:* rune.bredesen@matek.sintef.no (R. Bredesen).

0920-5861/00/$ – see front matter 
PII: S0920-5861(99)00289-8

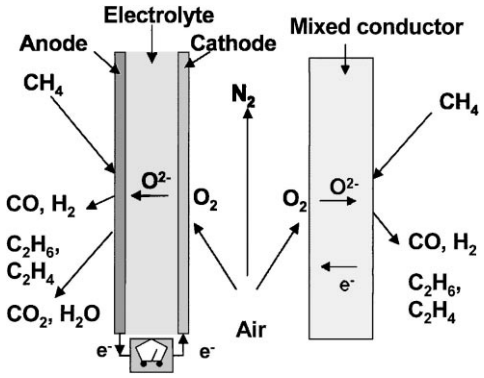


Fig. 1. Left: example of oxygen separation with an oxygen ion conducting electrolyte membrane (SOFC configuration); right: with a mixed conducting membrane.

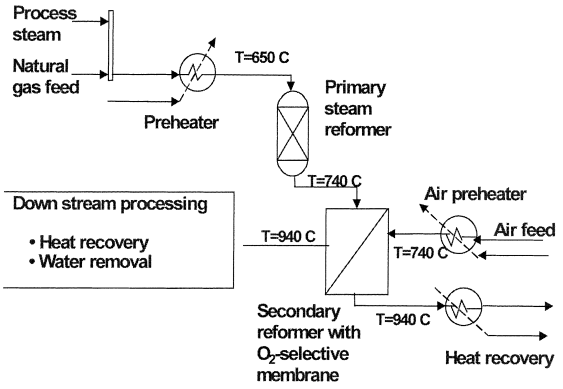


Fig. 2. Schematic flow sheet of combined reforming where an oxygen selective membrane supplies oxygen to the secondary reformer.

stability have been reported [1,2]. Currently, the most promising mixed conducting membrane materials are made from phases of the perovskite family; as the pure perovskites ($ABO_3$), the perovskite-like layered structure ($A_4B_6O_{13}$), and the brownmillerites ($A_2B_2O_5$). Membranes of these materials are reported to give oxygen fluxes in the range of 1–20 $cm^3\,cm^{-2}\,min^{-1}$ [1,2].

Oxygen selective membranes for production of pure oxygen have many possible applications in petrochemical, metallurgical, bleaching, combustion processes, in medicine, etc. One of the large oxygen consuming petrochemical processes is the production of synthesis gas ($CO + H_2$) from natural gas as an intermediate for synthesis of other bulk chemicals. Synthesis gas can be produced in different ways. In autothermal reforming of natural gas the heat required to maintain the endothermic steam reforming reaction is added by internal partial combustion by feeding oxygen to the reactor. The mixture of natural gas, water vapour and oxygen is equilibrated at 900–1000°C in a fixed bed. The reactor operates at typically 40 bar so a high pressure is needed to feed oxygen to the reactor. In the so-called combined reforming a portion of the natural gas (approximately 30–40%) is first steam reformed in a primary reformer, and then in a secondary reformer, the last part of the natural gas is combusted by mixing oxygen as in the autothermal reformer. The investment cost of the cryogenic oxygen plant is very high and constitutes about 35–45% and 25–35% of the total investment costs for autothermal and combined reforming, respectively [3]. An alternative to cryogenic oxygen production would be oxygen production by membranes. A membrane could be integrated with the reactor at high temperature, where the supply of oxygen is driven by the large partial pressure difference between the air side and natural gas side of the membrane. This is schematically illustrated in Fig. 2 for combined reforming.

One of the most promising mixed conducting oxygen membranes reported, showing oxygen fluxes higher than 10 $cm^3\,cm^{-2}\,min^{-1}$, is the so-called $SrFeCo_{0.5}O_x$ material, which is a mixed phase containing two main phases, $SrFe_{1-x}Co_xO_{3-z}$ and $Sr_4Fe_{6-x}Co_xO_{13}$ [4]. So far no studies have been reported which give a firm explanation of the defect structure and transport mechanism in this highly oxygen ion conducting material. Recent studies have, however, indicated that the chemical diffusion coefficient decreases with increasing Co content, which may suggest that the diffusion takes place by interstitial oxygen ions in the lattice [5]. The reason for such an assumption is that Co is more stable than Fe in the valence state 2+which disfavours interstitial diffusion.

It has, furthermore, been reported for many oxygen ion conducting materials that the surface reactions contribute significantly to the overall resistance to oxygen flow [6]. It is, therefore, of interest to study the surface reaction rates on the highly conducting materials. Knowledge about the rate limiting step in the overall mass transport could give guidelines for

further optimisation of these membranes and the operating conditions. In this study the surface exchange rate and the chemical diffusion coefficient in pure $Sr_4Fe_6O_{13}$, and in Ti- and La-doped material are determined by transient thermogravimetric measurements between 700 and 1000°C. La and Ti dopants may both act as donors in this material and are chosen as they may presumably increase the concentration of oxygen interstitials.

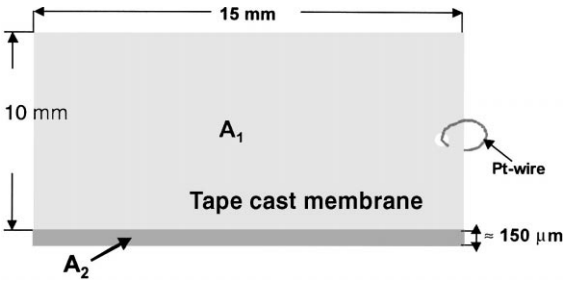


Fig. 3. Tape cast membrane sample.

## 2. Materials and methods

Powders of $Sr_4Fe_6O_{13}$ were made from powders of $SrCO_3$ (BDH Chemicals, purity > 99%) and $Fe_2O_3$ (Strem Chemicals, purity > 99.8%) which were mixed in a centrifugal ball mill using isopropanol as liquid medium. After milling the isopropanol was evaporated off and the mixture calcined at $1000 \pm 5$°C for 2 h. The calcined powder mixture was then milled in cyclohexane before a second calcination at $1000 \pm 5$°C was carried out. The powders of doped materials were made in the same way by partly substituting La for Sr and Ti for Fe. La was added in the form of $La_2O_3$ (Fluka, purity > 99.98%) and Ti in the form of $TiO_2$ (Merck, purity > 99%). The doped powders had the final stoichiometric compositions $Sr_{3.6}La_{0.4}Fe_6O_{13.2}$, $Sr_4Fe_{5.6}Ti_{0.4}O_{13.2}$, and $Sr_{3.6}La_{0.4}Fe_{5.6}Ti_{0.4}O_{13.4}$.

Slurries suitable for tape casting were made from the calcined powders using a standard procedure based on 2-butanone/ethanol azeotrope as solvent and poly(vinyl butyral) as binder. The slurry was tape cast on a glass plate using a height of the knife of 0.75 mm. After drying the green tape was calcined at $1180 \pm 5$°C for 5 h. The final thickness of the membranes was 120–170 μm.

The electrical conductivity was measured by the van Pauw method in one of the samples (La-doped material). The thermogravimetric measurements were carried out in a Setaram TGA 92 Thermoanalyser. A total of six or seven samples of tape cast membranes with dimension approximately $10 \times 15\,mm^2$ were hung on a single Pt wire in the balance, see Fig. 3. The individual membranes were separated by placing a thin 0.5 mm Pt wire between each. In the furnace the samples were located inside an alumina tube with an inner diameter of 16 mm. The gas inlet was located 20 cm from the hot zone of the furnace, and the gas was flowing at a rate of $300\,S\,cm^3\,min^{-1}$. The sample was treated in pure $O_2$, air, or in mixtures of Ar + air. The starting time of the experiment was corrected to account for the time needed for the gas to reach the sample.

The membrane phase composition was characterised by X-ray powder diffraction and the density by pycnometric measurements. The membrane thickness was determined in a scanning electron microscope.

The overall oxygen flux through a mixed conducting membrane operating in a chemical oxygen potential gradient will be determined by the chemical diffusion coefficient and the surface exchange rate coefficients. The total driving force for oxygen transport is the difference in oxygen partial pressure at the two sides of the membrane. A part of the driving force is used to support the bulk diffusion and the remaining to support the two surface reactions, see Figs. 4 and 5. During steady state conditions the rate of oxygen flow in

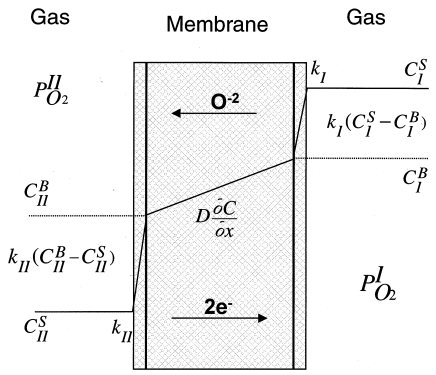


Fig. 4. Schematic illustration of loss in driving force by the bulk diffusion and the surface reactions in a membrane operation. $k$ = surface exchange rate constant, $C$ = concentration of oxygen, and $D$ = chemical diffusion coefficient.

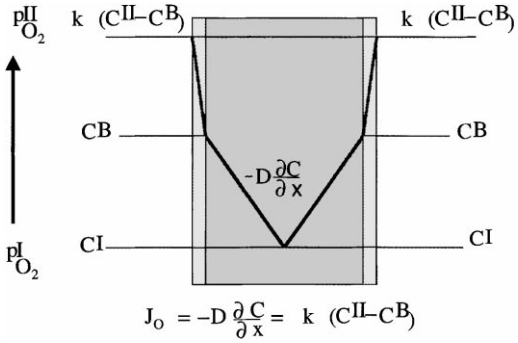


Fig. 5. Schematic illustration of loss in driving force by the bulk diffusion and the surface reactions in a transient thermogravimetric measurement. $k$ = surface exchange rate constant, $C$ = concentration of oxygen, $D$ = chemical diffusion coefficient, and $J_O$ = oxygen flux.

the membrane bulk and the exchange rates at the surfaces are equal.

In a transient thermogravimetric measurement the membrane is first equilibrated at a certain partial pressure of oxygen. The oxygen partial pressure is then rapidly changed to a nearby value, and the change in the membrane weight is measured as a function of time. The weight change corresponds to a net transport of oxygen into the membrane (weight increase) or out of the membrane (weight loss). The rate of weight change will depend on the rate of oxygen diffusion in the membrane and the rate of oxygen exchange on the surface.

In transient thermogravimetric measurements it is possible to study surface reaction kinetics in both directions, i.e., either uptake of oxygen or liberation of oxygen to the surroundings. Only results of the rate of oxygen uptake by the sample will be reported here.

For a one-dimensional model with transport normal to the surface $A_1$ (assuming $A_1 \gg A_2$, see Fig. 3), the following expression may be given [7]:

$$\frac{M_t}{M_\infty} = 1 - \sum_{n=1}^{\infty} \frac{2L^2 \exp\left(-b_n^2 Dt/l^2\right)}{b_n^2(b_n^2 + L^2 + L)}, \qquad (1)$$

where $M_t$ denotes the weight change from start to time $t$, and $M_\infty$ the total weight change observed in the experiment. $L = lk/D$, where $k$ is the surface exchange rate constant, $D$ the chemical diffusion coefficient and $l$ is half the thickness of the membrane. $b_n$ are positive roots of the equation $b \tan b = L$ [8].

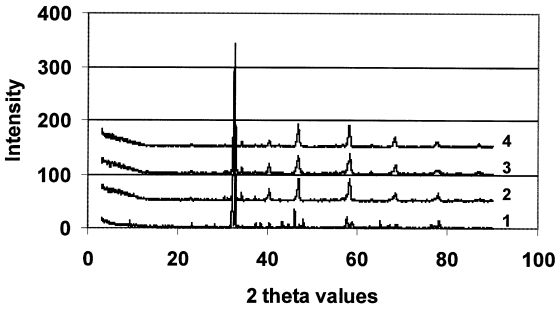


Fig. 6. XRD patterns of powders made from tape cast membranes: (1) undoped membrane, (2) Ti + La-doped membrane, (3) La-doped membrane, and (4) Ti-doped membrane.

It may be noted that the $D$ referred to here expresses the effective diffusivity of the rate limiting defect, assumed to be an oxygen defect. In a mixed conducting material $D$ will be higher than the oxygen tracer and the self-diffusion coefficients ($D^*$ and $D_o$, respectively) due to the simultaneous electron diffusion. The value of $D$ will depend on the mobility of the oxygen defects and a thermodynamic factor [9].

## 3. Results

The XRD patterns of powders of tape cast membranes are shown in Fig. 6. The density measurements showed that the closed porosity in the membranes was in the range 10–15%.

Fig. 7 shows some examples of the measured weight change to the total weight change, $(M_t/M_\infty)$ as a function of time, and the fitting of the model, given by Eq. (1), to determine $D$ and $k$.

In Fig. 8 the obtained values for $D$ at 700–1000°C are shown. These results correspond to the values of $D$ when the samples are first equilibrated in air and the gas is changed to pure oxygen. The values of $D$ for the different compositions are comparable in magnitude, and the apparent activation energies fall in the range of 50–130 kJ mole$^{-1}$.

In Fig. 9 the values of the surface exchange reaction rate constant $k$ are shown for experiments where the ambient gas is changed from air to pure oxygen. The values of $k$ obtained by fitting the model in Eq. (1) are nearly constant as a function of temperature; however, a slight tendency of $k$ decreasing with increasing temperature may be observed. The obtained values of $D$ and $k$ suggest

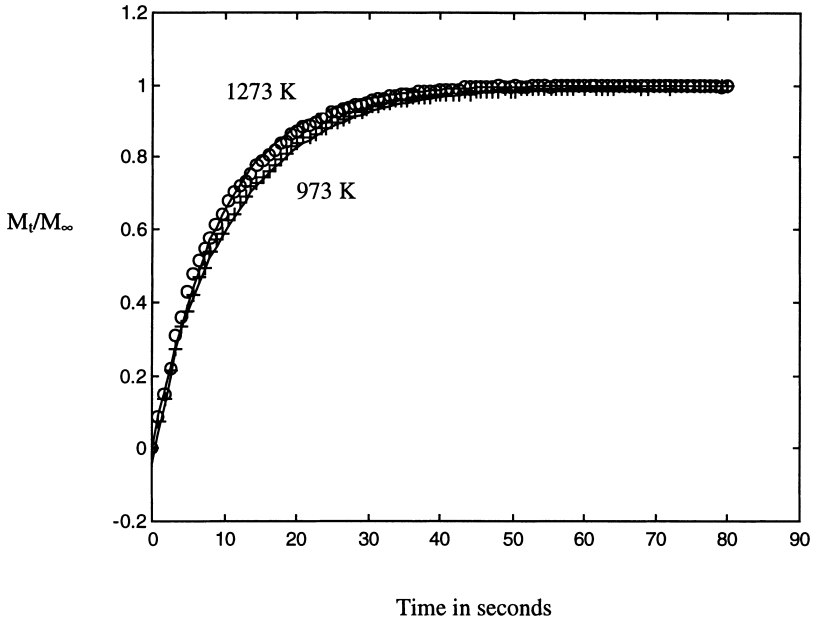


Fig. 7. Examples of measured weight change at time $t$ ($M_t$) relative to total weight change ($M_\infty$) as a function of time transient thermogravimetric experiments. The model in Eq. (1) has been fitted to the experimentally obtained curve.

that the rate of the surface reaction is rate limiting only during the first few seconds of the experiments. The sensitivity to variations in $k$ is, therefore, rather low when the complete weight change curve is used in the fitting of the model. The values of $k$ were, therefore, also estimated only from the initial gradient of the weight change curves by assuming $k = (J_O/(C^{II} - C^I))_{\lim t \to 0}$, where $J_O$ is the flux of oxygen, and $C^{II}$ and $C^I$ concentration of oxygen in pure oxygen and air, respectively. The values of $k$ obtained by this method are shown in Fig. 10, and in this case $k$ is increasing slightly with temperature.

In Fig. 11 the measured weight change when the ambient gas is changed from air to pure oxygen is shown as a change in the average oxygen content in the

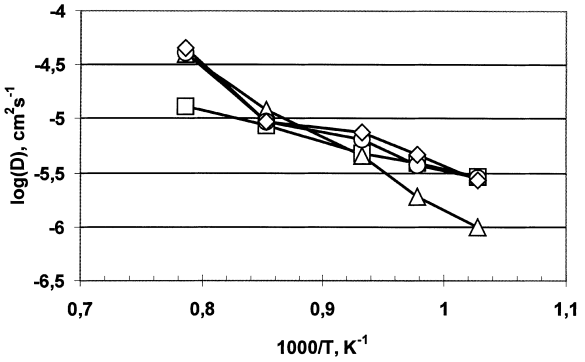


Fig. 8. Values of the chemical diffusion coefficient as a function of reciprocal temperature obtained by changing the ambient gas from air to pure oxygen: (□) $Sr_4Fe_6O_{13}$, (Δ) $Sr_{3.6}La_{0.4}Fe_6O_{13.2}$, (○)$Sr_4Fe_{5.6}Ti_{0.4}O_{13.2}$, (◇)$Sr_{3.6}La_{0.4}Fe_{5.6}Ti_{0.4}O_{13.4}$.

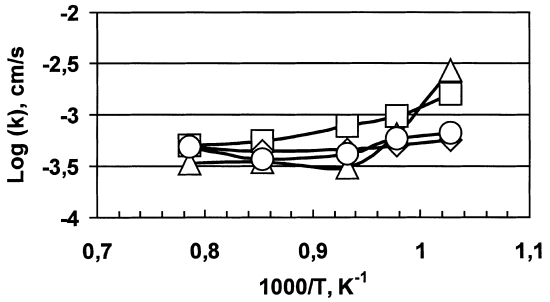


Fig. 9. Values of the surface exchange reaction rate constant obtained by best fit of Eq. (1) in experiments where the ambient gas is changed from air to pure oxygen as a function of the reciprocal temperature: (□) $Sr_4Fe_6O_{13}$, (Δ) $Sr_{3.6}La_{0.4}Fe_6O_{13.2}$, (○) $Sr_4Fe_{5.6}Ti_{0.4}O_{13.2}$, and (◇) $Sr_{3.6}La_{0.4}Fe_{5.6}Ti_{0.4}O_{13.4}$.

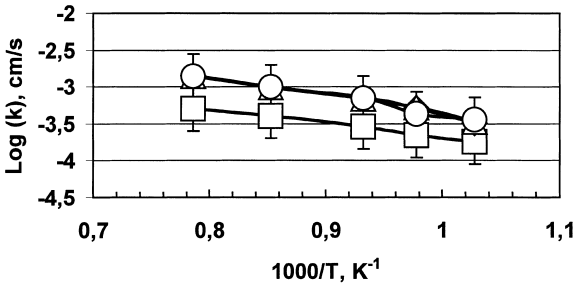


Fig. 10. Values of the surface exchange reaction rate constant obtained by estimating $J_O/(C^{II}-C^{I})_{\lim t\to 0}$ in experiments where the ambient gas is changed from air to pure oxygen as a function of the reciprocal temperature: (□) $Sr_4Fe_6O_{13}$, (Δ) $Sr_{3.6}La_{0.4}Fe_6O_{13.2}$, (○)$Sr_4Fe_{5.6}Ti_{0.4}O_{13.2}$, and (◇) $Sr_{3.6}La_{0.4}Fe_{5.6}Ti_{0.4}O_{13.4}$.

sample. It has for simplicity been assumed that the starting compositions equilibrated in air are stoichiometric compositions, i.e., $Sr_4Fe_6O_{13}$, $Sr_{3.6}La_{0.4}Fe_6O_{13.2}$, $Sr_4Fe_{5.6}Ti_{0.4}O_{13.2}$, $Sr_{3.6}La_{0.4}Fe_{5.6}Ti_{0.4}O_{13.4}$, respectively. The results show that the increase in oxygen concentration is larger for the La-doped samples compared to the Ti-doped, and that undoped material has the lowest increase in oxygen concentration.

Some further studies were carried out on the La-doped material. For this sample the total weight change was measured for different steps in partial pressure of oxygen. In all experiments the final partial pressure was 1 atm oxygen, while the starting pressure was varied. The results are given in Table 1. The results show that the oxygen content increases sharply at high oxygen partial pressures, but is relatively invariable at lower pressures.

Also the conductivity of the La-doped material was measured as a function of the partial pressure of oxygen at 1000°C. The results are given in Fig. 12. The measurements started at room temperature and high oxygen pressure. It was observed that after reaching the temperature at 1000°C the conductivity decreased slowly with time. The initial high conductivity is shown by the two points well above the others. When the conductivity reached a constant value the change measured as a function of the oxygen partial pressure is close to the relationship $\mathrm{Log}\,G \propto \frac{1}{4}\mathrm{Log}(P_{O_2})$ at high oxygen pressures. At lower oxygen pressures the conductivity seems to flatten out towards a region of small oxygen partial pressure dependency.

## 4. Discussion

### 4.1. XRD-analysis

Interpretation of phase compositions only based on XRD patterns is uncertain for these types of materials due to different phases having more or less overlapping patterns. However, from the results in Fig. 6, it appears that a single phase of $Sr_4Fe_6O_{13}$ has been formed in the undoped membrane. The doped materials show broader peaks, and are therefore more difficult to interpret. These membranes also have some weak peaks at approximately $2\theta = 30.3$ and 34.2, which can be interpreted as $SrFe_{12}O_{19}$. Based on these results the doped materials seem less homogeneous than the undoped.

### 4.2. Chemical diffusion coefficient

The values of the chemical diffusion coefficient obtained from the transient thermogravimetric measurements are about one order of magnitude higher than those obtained in the so-called $SrFeCo_{0.5}O_z$ by transient conductivity measurements [10]. $SrFeCo_{0.5}O_z$ is a multiphase material consisting mainly of $Sr_4Fe_{6-x}Co_xO_{13}$ and $SrFe_{1-x}Co_xO_{3-z}$. Furthermore, as previously mentioned, it has been shown that the value of $D$ increases with decreasing Co content. In light of these results, it is not surprising that the value of $D$ is higher in the undoped material. A possible explanation for this result could be that the $Co^{3+}$ ions have a greater tendency to be reduced to the valence state 2+than the $Fe^{3+}$ ions. Such reduction in valence state would disfavour the concentration of interstitial oxygen ions, which have been suggested to be the mobile oxygen species [10]. Fig. 13 shows a possible defect model for the $Sr_4Fe_6O_{13}$ material.

The effect of the doping on the value of $D$ is minor. This suggests that the major defect transporting oxygen is the same as in the undoped material and that the mobility of this defect is largely unaltered. An idea about the change in oxygen content when changing the ambient gas from air to oxygen can be obtained from Fig. 11. As seen, the change in nonstoichiometry is comparable with the change obtained by doping. This suggests that the concentration of inherently formed oxygen interstitials must be of the same magnitude or higher than what is formed by doping.

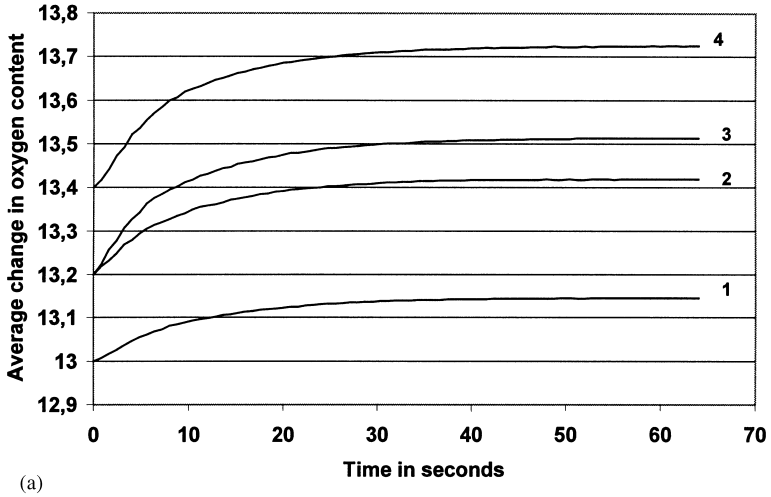


(a)

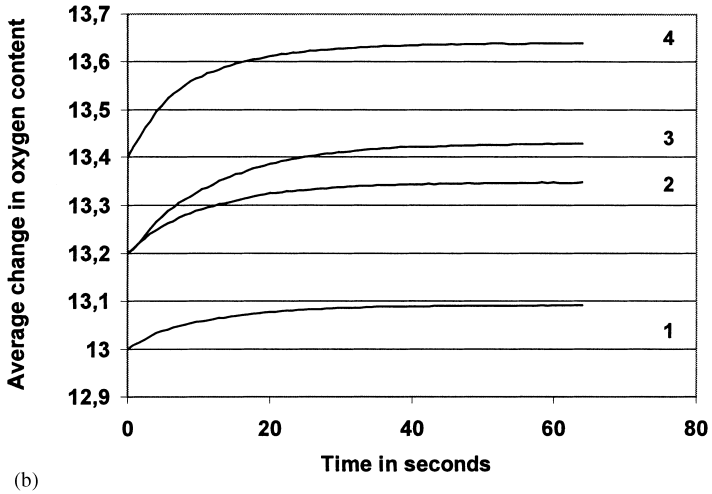


(b)

Fig. 11. (a): Average oxygen content in the membrane material as a function of time in transient thermogravimetric measurements at 1000°C when the ambient gas is changed from air to pure oxygen. As a reference value it has been assumed that the membranes have stoichiometric compositions in air: (1) $Sr_4Fe_6O_{13}$, (2) $Sr_4Fe_{5.6}Ti_{0.4}O_{13.2}$, (3) $Sr_{3.6}La_{0.4}Fe_6O_{13.2}$, and (4) $Sr_{3.6}La_{0.4}Fe_{5.6}Ti_{0.4}O_{13.4}$; (b): Average oxygen content in the membrane material as a function of time in transient thermogravimetric measurements at 700°C when the ambient gas is changed from air to pure oxygen. As a reference value it has been assumed that the membranes have stoichiometric compositions in air: (1) $Sr_4Fe_6O_{13}$, (2) $Sr_4Fe_{5.6}Ti_{0.4}O_{13.2}$, (3) $Sr_{3.6}La_{0.4}Fe_6O_{13.2}$ and (4) $Sr_{3.6}La_{0.4}Fe_{5.6}Ti_{0.4}O_{13.4}$.

Table 1
Total weight change (mg) in La-doped material when the partial pressure of oxygen is changed from various starting values to 1 atm oxygen (volume of sample = 0.093 $cm^3$)

| Temperature, $T$ (°C) | Start pressure (atm) | | | | |
|---|---|---|---|---|---|
| | $P_{O_2} = 0.0165$ | $P_{O_2} = 0.042$ | $P_{O_2} = 0.064$ | $P_{O_2} = 0.097$ | $P_{O_2} = 0.2$ |
| 1000 | 3.86 | 3.73 | 3.91 | 3.9 | 2.5 |
| 900 | 4.17 | 4.09 | 4.13 | 3.98 | 2.36 |

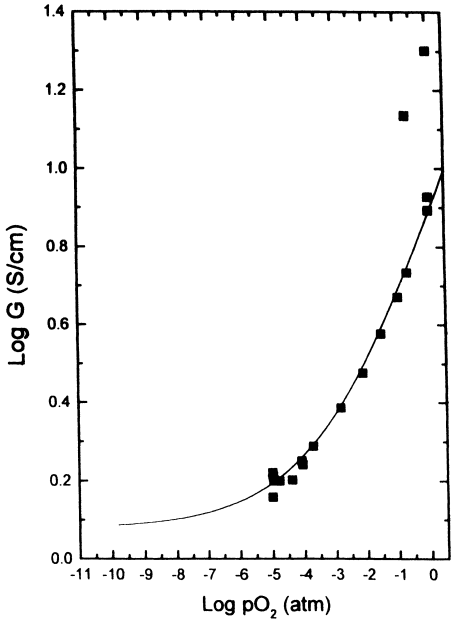


Fig. 12. The electrical conductivity of La-doped material as a function of the partial pressure of oxygen at 1000°C. The conductivity at high partial pressures of oxygen has close to a $P_{O_2}^{1/4}$ dependence. The two points with high conductivity at high oxygen pressure may possibly represent a metastable state.

The neutrality condition for the defects in the doped material is

$$2\lfloor V_{O^{\cdot\cdot}}\rfloor + p + [Mf_M^{\cdot}] = 2[O_i^{''}] + n, \quad (2)$$

where $Mf_M^{\cdot}$ is a dopant ion (La and/or Ti) substituting Sr and/or Fe. If the concentration of dopants is too low to determine the concentration of interstitial oxygen, the neutrality conditions can be approximated by the same conditions as for the undoped material, i.e.,

$$\lfloor V_{O^{\cdot\cdot}}\rfloor = [O_i^{''}], \quad (3)$$

at intermediate and

$$p = 2\left\lfloor O_i^{''}\right\rfloor, \quad (4)$$

at high oxygen pressures. A weight increase in the region where the neutrality condition is determined by the oxygen point defects may be explained by Eq. (2). In this region the electron hole concentration will increase proportional to $P_{O_2}^{1/4}$, and in order to keep electroneutrality a small reduction in the concentration of oxygen vacancies and an increase in the concentration of oxygen interstitials may take place:

$$\tfrac{1}{2}O_2 + V_{O^{\cdot\cdot}} = O_O^X + 2h^{\cdot}, \quad (5)$$

$$\tfrac{1}{2}O_2 = O_i^{''} + 2h^{\cdot}. \quad (6)$$

The results from the electrical conductivity measurements of the La-doped material suggest that the conductivity has a $P_{O_2}^{1/4}$ dependency at high oxygen partial pressures, see Fig. 12. Combined with the results given in Fig. 11, this suggests that the dominating defects in air are the inherently formed oxygen Frenkel point defects. Since the dissolution of oxygen is higher in La-doped materials when the ambient atmosphere is changed from air to 1 atm oxygen, this also suggests that the concentration of electron holes is higher in this material. This is supported by the observation that the electrical conductivity is higher in La-doped material than in the undoped material [11]. A simple estimate of the concentration of oxygen interstitials can be made by assuming that the concentration is approaching an oxygen partial pressure dependence of $\mathrm{Log}([O_i^{\cdot\cdot}]) \propto \frac{1}{6}\mathrm{Log}(P_{O_2})$ in the partial pressure region from air to 1 atm oxygen. The weight change from air to pure oxygen in Table 1 would then correspond to such a variation. From this the concentration of interstitial oxygen ions can be estimated as shown in Fig. 14 for the different measurements. As seen the estimated concentration is significantly higher than the concentration of interstitial oxygen expected from doping with La. It should be mentioned that in the region where $\mathrm{Log}\, p \propto \frac{1}{4}\mathrm{Log}(P_{O_2})$, see Fig. 12, the change in the concentration of interstitial oxygen is relatively even smaller than what was assumed in the estimate given in Fig. 14. Thus, the concentration level estimated in Fig. 14 represents a minimum level for the concentration of interstitial oxygen defects. This result supports the assumption that the inherently formed oxygen defect concentration is higher than the dopant concentration.

### *4.3. Surface exchange reaction rate constant*

The surface exchange reaction rate constant does not change very much with temperature. However, the results from the fitting using Eq. (1) give a different tendency than when only the initial rate is estimated. At this stage it is not possible to give a more

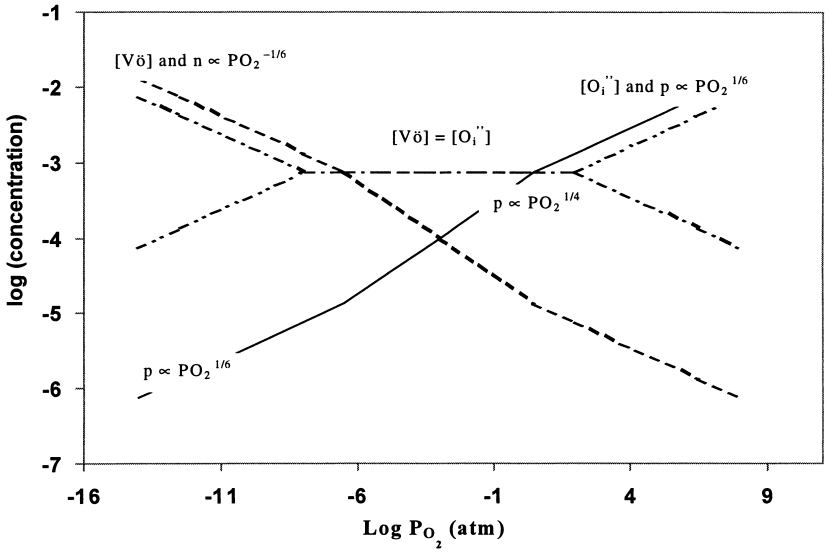


Fig. 13. Diagram showing the variation in the logarithm of the defect concentrations as a function of the logarithm of the partial pressure of oxygen for an undoped oxide with Frenkel defects in the oxygen sublattice (arbitrary example).

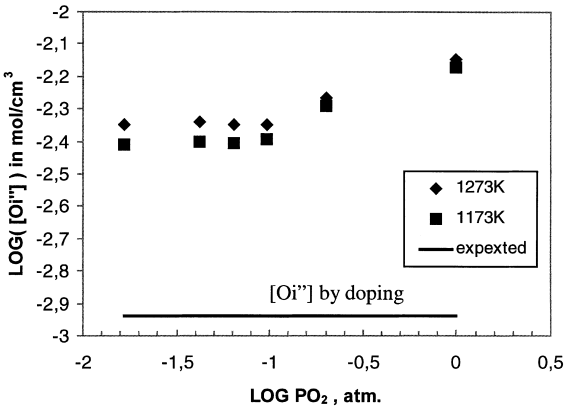


Fig. 14. Calculated concentration of interstitial oxygen (mole $cm^{-3}$) in La-doped material from the total weight change (Table 1) when the ambient gas is changed from various low partial pressures to 1 atm oxygen. The results have been fitted by assuming that the change in concentration of oxygen interstitials from air to oxygen is proportional to $P_{O_2}^{1/6}$.

detailed explanation of the surface reaction mechanism. The surface reaction rate may depend on different parameters as, for instance, the splitting of the oxygen molecule, the concentration of particular sites or species on the surface or defects in the lattice, uptake of electrons, incorporation of the oxygen into the lattice, etc. In a previous study it has been suggested that the small amount of $CO_2$ in air may cause surface modifications on $SrCo_{0.8}Fe_{0.2}O_{3-z}$ which resulted in a reduced oxygen flux through the membrane when air was used as the high oxygen pressure side [12]. Such an effect could also be important for the obtained results of *k* in this study. However, further studies are needed to investigate a possible effect of $CO_2$ traces in air.

The ratio of *k/D* is approximately two orders of magnitude, which suggests that the surface reaction rate has an importance for the overall incorporation of oxygen only during the very first stage of the reaction. In further studies *k* should also be measured as a function of the oxygen partial pressure. This would give information about the oxygen pressure dependency of the surface reaction exchange rate.

### *4.4. Electrical conductivity*

The oxygen partial pressure dependence of the electrical conductivity is similar to what can be expected for electron holes in an oxygen partial pressure region where the concentration of interstitial oxygen ions is fixed, see Fig. 13. When the oxygen pressure is reduced the electrical conductivity appears to approach a typical minimum with a significant contribution of oxygen ions to the total conductivity. Compared to the observed conductivity of the undoped material [11]

the minimum value of the conductivity is higher, and furthermore, located at a lower partial pressure of oxygen. This, therefore, suggests that the La-doping has increased both the electron hole conductivity as well as the ionic conductivity. This is not easy to explain from the defect model given in Fig. 13 by simple doping reactions. The results may suggest that the material is not a pure phase, but a multiphase material as indicated by the XRD results. Alternatively, the material formed by doping is a "new" material with higher concentrations of inherently formed oxygen interstitials and electron holes under similar ambient conditions compared to undoped $Sr_4Fe_6O_{13}$. Thus, the La-doping may have increased the equilibrium constants for the Frenkel defect pair formation and/or for oxidation (Eq. (6)).

## 5. Summary

The results of the transient thermogravimetric measurements in $Sr_{4-x}La_xFe_{6-y}Ti_yO_{13+[(x+y)/2]}$ show that the chemical diffusion coefficient, as measured when the ambient atmosphere is changed from air to 1 atm oxygen, is in the range of $1 \times 10^{-6} - 4 \times 10^{-5}\,cm^2\,s^{-1}$ in the temperature range 700–1000°C. The estimated activation energy of $D$ is in the range of 50–130 kJ mol$^{-1}$. The surface exchange reaction rate constant in the same temperature range varies from $2 \times 10^{-3}\,cm\,s^{-1}$ to $2 \times 10^{-4}\,cm\,s^{-1}$ for the incorporation of oxygen when the gas is changed from air to 1 atm oxygen. The electrical conductivity has a $\mathrm{Log}\,\sigma \propto \frac{1}{4}\mathrm{Log}(P_{O_2})$ at high oxygen pressures which is assumed to reflect electron hole conductivity. A transition towards a minimum in conductivity is observed at low partial pressures of oxygen. The electrical conductivity is higher in La-doped material than in pure, as well as the concentration of oxygen point defects. This feature is possibly a result of formation of a new material. This could either be a multiphase material or a material with higher concentrations of inherently formed oxygen and electronic defects.

## References

[1] A.C. Bose, G.J. Stiegel, A.F. Sammells, in: Proceedings of the Fifth International Conference on Inorganic Membrane, Nagoya, Japan, 22–26 June 1998, pp. 6–9.
[2] U. Balachandran, P.S. Maiya, B. Ma, J.T. Dusek, R.L. Mieville, J.J. Picciolo, Development of mixed-conducting ceramic membranes for converting methane syngas, in: R. Bredesen (Ed.), Proceedings of the Fourth Workshop on Catalytic Membrane Reactors, Oslo, Norway, 30–31 May 1997, pp. 15–26.
[3] R. Bredesen, J. Sogge, in: Paper presented at: The United Nations Economic Commission for Europe Seminar on Ecological Applications of Innovative Membrane Technology in Chemical Industry; Chem/Sem. 21/R.12, Cetraro, Calabria, Italy, 1–4 May 1996.
[4] H. Fjellvåg, B.C. Hauback, R. Bredesen, J. Mater. Chem. 7 (12) (1997) 2415–2419.
[5] R. Bredesen, H. Ræder, C. Simon, A. Holt, in: Proceedings of the Fifth International Conference on Inorganic Membrane, Nagoya, Japan, 22–26 June 1998, pp. 412–415.
[6] H.J.M. Bouwmeester, H. Kruidhof, A.J. Burggraaf, Solid State Ionics 72 (1994) 185–194.
[7] J. Crank, The Mathematics of Diffusion, Oxford Science Publications, Oxford, 1975, pp. 61–62.
[8] Carslaw, Jaeger, Conduction of Heat in Solids, Oxford Science Publications, Oxford, 1959, p. 491.
[9] J. Maier, Solid Sate Ionics 112 (1998) 197–228.
[10] B. Ma, U. Balachandran, J.-H. Park, C.U. Segre, Solid State Ionics 83 (1996) 65–71.
[11] Unpublished results.
[12] L. Qiu, T.H. Lee, L.-M. Liu, Y.L. Yang, A.J. Jacobson, Solid State Ionics 76 (1995) 321–329.